ORGANIC PROCESS RESEARCH & DEVELOPMENT
OPR&D

pubs.acs.org/OPRD Article

Synthesis of Rovafovir Etalafenamide (Part IV): Evolution of the Synthetic Process to the Fluorinated Nucleoside Fragment

David A. Siler,* Selcuk Calimsiz, Ian J. Doxsee, Bernard Kwong, Jeffrey D. Ng, Keshab Sarma, Jinyu Shen, Jonah W. Curl, Jason A. Davy, Jeffrey A. O. Garber, Sura Ha, Olga Lapina, Jisung Lee, Lennie Lin, Sangsun Park, Mary Rosario, Olivier St-Jean, and Guojun Yu

Cite This: *Org. Process Res. Dev.* 2021, 25, 1263−1274 Read Online

ACCESS | Metrics & More | Article Recommendations | Supporting Information

ABSTRACT: Fluorinated nucleoside **1** is a key starting material in the synthesis of rovafovir etalafenamide (**2**), a novel nucleotide reverse transcriptase inhibitor under development at Gilead Sciences for the treatment of HIV. While an initial manufacturing route enabled the production of **1** to support clinical development, alternative approaches were explored to further enhance manufacturing effectiveness, improve processing time, reduce cost, and minimize the environmental impact. Toward this end, two new routes were developed to a key synthetic intermediate, which was converted to **1** using a new protecting group strategy. The new chemistry led to improvements in the manufacturing process while reducing the overall process mass intensity (PMI).

KEYWORDS: *fluorinated nucleoside, glycosylation, fluorination, enzymatic hydrolysis*

INTRODUCTION

Synthetic nucleoside and nucleotide analogues have played a prominent role in the treatment of a variety of conditions, including viral infections.[1] Fluorinated nucleosides and nucleotides, in particular, have received attention as the incorporation of fluorine into these structures can improve their biological activity and stability.[2,3] Rovafovir etalafenamide (**2**, Scheme 1), a fluorinated nucleotide analogue of 2′,3′-didehydro-2′,3′-dideoxy adenosine (d4AP), maintains the anti-HIV activity of the nonfluorinated analogue while exhibiting lower mitochondrial toxicity and is being developed for the treatment of HIV.[4] The accompanying articles in this issue describe the synthesis of **2** via a convergent synthesis which combines the fluorinated nucleoside core **1** and the phosphonamidate ester **3**.[5] The development of a manufacturing process for the nucleoside core is described herein.

Scheme 1. Retrosynthetic Approach to 2

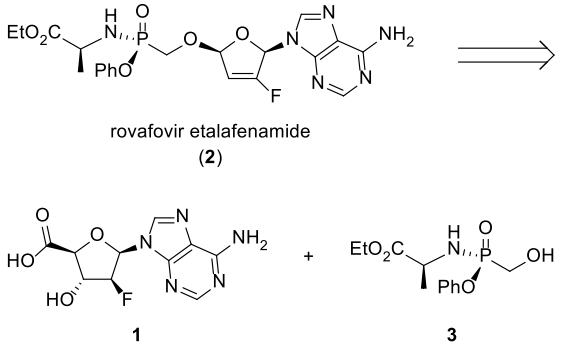

An initial manufacturing route for **1** is shown in Scheme 2.[6] In this route, the advanced fluoro glycosyl benzoate **4** (prepared via several steps[7]) was brominated at the anomeric position. From bromide **5**, a subsequent glycosylation reaction with N^6-benzoyladenine (**6**) afforded **7**, which was then selectively debenzoylated to give the first isolated intermediate, diol **8**. Bis-silylation of **8** followed by a moderately selective deprotection of the 5′-silyl ether yielded **10** in a telescoped sequence. Following oxidation to **11**, a final global deprotection afforded **1**. This manufacturing route provided **1** with an overall yield of 41%, enabling the production of sufficient amounts of **1** to support the clinical development of **2**.

Several areas for improvement of the route, however, were noted. Specifically, the selective ester hydrolysis of **7** required careful control of the stoichiometry and reaction temperature to avoid overhydrolysis of the benzamide moiety, while the subsequent workup and crystallization of **8** were solvent- and time-intensive. As selective direct oxidation of the 5′-OH group was found to be challenging, the two-step sequence consisting of bis-silylation followed by deprotection was developed; this approach contributed to lengthy manufacturing operations and high overall process mass intensity (PMI)[8] for **10**. Additionally, the lability of the silyl ether functionality resulted in the formation of significant amounts of **8** along with **10**, which not only led to an erosion in yield but also impacted the downstream oxidation reaction, workup, and isolation.

Received: January 21, 2021
Published: May 7, 2021

Scheme 2. Initial Manufacturing Route for 1[a]

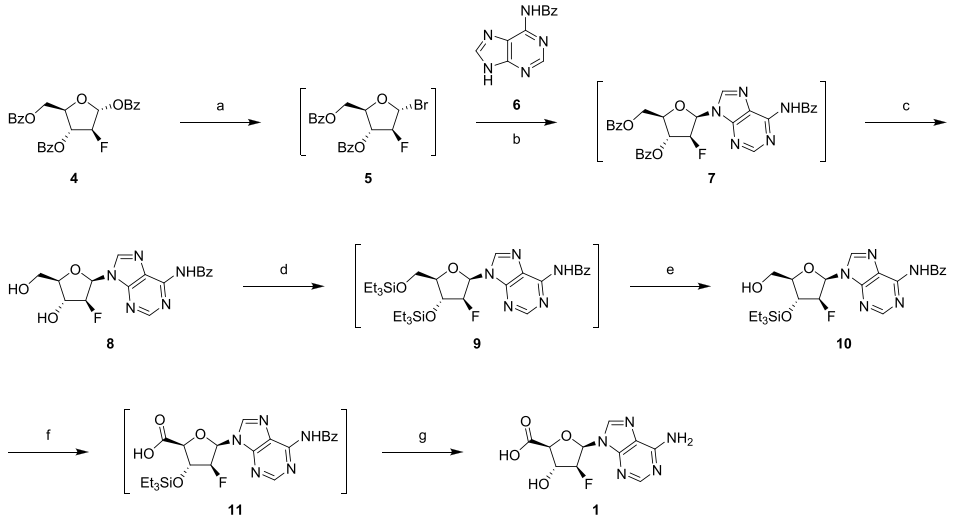

[a]Reagents and conditions: (a) 33 wt % HBr in AcOH, CH_2Cl_2, 0 °C; (b) tetrahydrofuran (THF), *N*-methyl-2-pyrrolidone (NMP), 68 °C; (c) NaOH, THF, H_2O, 0 °C, 59% from **4**; (d) Et_3SiCl, iPr_2NEt, PhMe, 50 °C; (e) TsOH·H_2O, MeOH, 3 °C, 73% from **8**; (f) $PhI(OAc)_2$, (2,2,6,6-tetramethylpiperidin-1-yl)oxidanyl (TEMPO), Na_2HPO_4, MeCN, H_2O, 22 °C; and (g) 25 wt % NaOMe in MeOH, MeOH, 22 °C, 96% from **10**.

Scheme 3. New Synthetic Strategy for the Manufacturing of 1

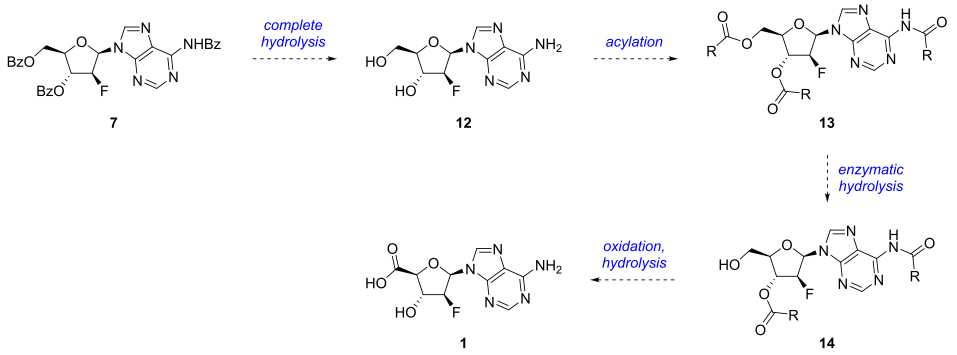

RESULTS AND DISCUSSION

New Route Design. To address the difficulties with the initial manufacturing process described above, a new synthetic route to **1** was developed that leveraged the process knowledge gained from the initial route. In this new route (Scheme 3), global hydrolysis of **7** to new intermediate **12** would obviate the need for careful control of a selective deprotection. From **12**, protection of the 3′-OH as an ester in place of the silyl ether was envisioned for several reasons: (1) the acylation reaction would be compatible with the free amino group on the adenine moiety; (2) the resulting ester functionality is expected to have improved chemical stability under the subsequent processing conditions relative to the analogous silyl ether; and (3) enzymatic hydrolysis could be leveraged to access intermediate **14**.

Improved Glycosylation Process/Global Debenzoylation to 12. The new route development began with the refinement of the telescoped glycosylation step that forms **7** (Scheme 4). Following this sequence, **4** was first converted to glycosyl bromide **5** with excellent diastereoselectivity (only the α-diastereomer is observed via ^{19}F nuclear magnetic resonance (NMR)). After aqueous workup and drying, **5** was reacted with a large excess of **6** (2.2 equiv) which also acts as a base to scavenge the HBr produced during the reaction. The glycosylation reaction is very sluggish, partly due to the low solubility of **6** in the reaction mixture. Efforts to increase the solubility of **6**, and therefore increase the reaction rate, using more polar reaction solvents led to a decrease in diastereoselectivity (Table 1), likely due to a change in the reaction mechanism.[9] For this reason, the glycosylation reaction medium remained unchanged in the new route (32:1 THF/NMP), affording a 95:5 mixture of anomers favoring the β-diastereomer on scale.[10] Inefficiencies in the reaction workup, however, provided opportunities for develop-

Scheme 4. Telescoped Route to 12 from 4[a]

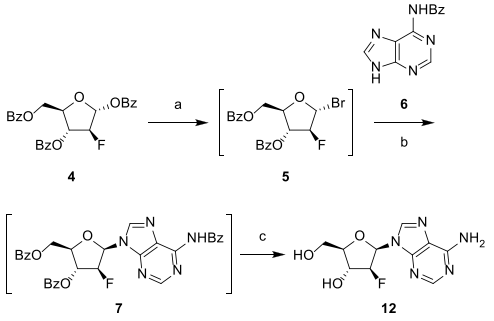

[a]Reagents and conditions: (a) 33 wt % HBr in AcOH, CH_2Cl_2, 0 °C; (b) THF, NMP, 68 °C; and (c) LiOH, MeOH, H_2O, 22 °C, 61% from **4**.

https://doi.org/10.1021/acs.oprd.1c00026
Org. Process Res. Dev. 2021, 25, 1263−1274

Table 1. Impact of the Solvent on the Glycosylation of 5[a]

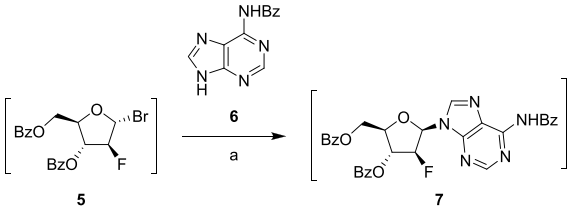

entry	solvent	ratio (β/α)
1	THF	95.2:4.8
2	THF/NMP (73:1)	94.0:6.0
3	THF/NMP (23:1)	93.8:6.2
4	THF/NMP (14:1)	92.6:7.4
5	THF/NMP (7:1)	91.6:8.4

[a]Reagents and conditions: (a) THF, NMP (solvent ratio indicated in the table), 68 °C.

ment. In the initial manufacturing process, a lengthy workup procedure was used, including (1) filtration of the reaction mixture to remove the majority of the excess **6** as the corresponding HBr salt, (2) solvent exchange of the filtrate from THF to dichloromethane to facilitate the subsequent aqueous workup, (3) acidic aqueous workup to remove the remaining **6**, and (4) solvent exchange of the organic layer from dichloromethane back to THF for compatibility with the downstream debenzoylation conditions. Overall, these solvent exchanges contributed to an increase in processing time, cost, and waste. To streamline the workup, it was found that the THF-rich filtrate (after glycosylation and filtration) could be washed directly with a mixture of dilute HCl and brine to efficiently remove residual **6**, obviating the need for solvent exchanges.

With the workup addressed, the hydrolysis reaction conditions were modified to allow for the complete hydrolysis of **7**. Simply increasing the reaction temperature from 0 to 50 °C led to full conversion to **12**, but product decomposition was also observed. After additional screening, methanol was identified as a beneficial cosolvent, improving the reaction rate while allowing for the reaction to be performed at a lower temperature (22 °C). Upon reaction completion, the mixture was acidified with aqueous HCl, with **12** partitioning into the aqueous layer due to its high solubility in water at low pH. This operation enabled the rejection of many process impurities in the organic layer, including the stoichiometric byproduct benzoic acid. With these conditions, however, precipitation of sodium chloride was observed during the workup due to the presence of methanol in the aqueous layer. A change in the base from sodium hydroxide to lithium hydroxide in the hydrolysis step improved the workup as lithium chloride is more soluble in methanol-rich water; gratifyingly, this change provided an increase in the reaction rate as well. After workup, **12** could be crystallized from the aqueous layer by first neutralizing to pH 6−8 and then removing residual methanol by distillation. The new route provided **12** in 61% isolated yield from **4** on kilogram scale (compared to 59% isolated yield of **8** from **4** in the initial route). While the PMI for this three-step telescoped process was increased by 27% relative to the original route, this increase is primarily due to an increased use of water; the solvent contribution to the PMI is reduced by 15%. In addition, the simplification of the workup for intermediate **7** and the direct crystallization of **12** from the aqueous medium reduced the processing time of the telescoped process. The glycosylation step produces 5−6% AN (area normalized) of the α-anomer impurity, but this impurity is effectively purged to levels of 0.1−0.4% AN in the crystallization of **12**. Based on X-ray crystallography data (Figure 1), a

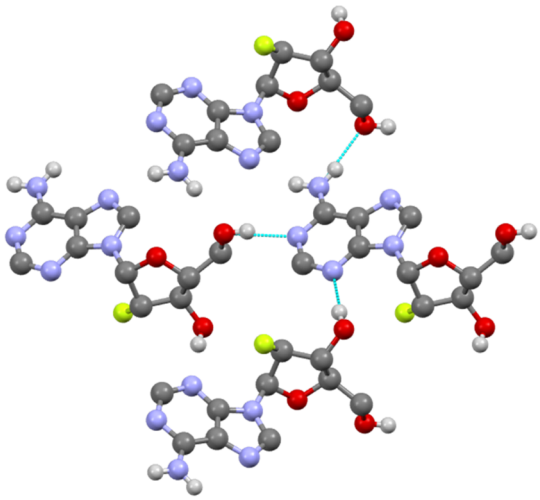

Figure 1. Three-dimensional hydrogen bond network for **12** (single-crystal X-ray structure).

significant hydrogen bonding network exists between molecules of **12** in the solid state, including H-bonds between the 3′-OH and a neighboring N3 and between the 5′-OH and a neighboring 6-NH_2. This high degree of intermolecular bonding interactions provides a possible explanation for the high crystallinity of **12** as well as the effective purge of the α-anomer impurity, which is unable to participate in this H-bonding network to the same extent.

Alternative Route to 12 from Adenosine. Although the modifications to the glycosylation sequence enabled a robust synthesis of **12**, an alternative route was investigated (Scheme 5) to eliminate the time-consuming glycosylation sequence and reduce the number of chemical steps (including the steps required to prepare starting material **4**). This alternative route would make use of adenosine (**15**), a relatively inexpensive starting material, but the challenges of selective protection of the 3′-OH and 5′-OH and subsequent fluorination of the 2′ position would need to be addressed.

At the outset, the protection of the 3′ and 5′ hydroxy groups as the corresponding benzoyl esters was explored to eventually intercept intermediate **12**. This could be accomplished via selective deprotection of tri-*O*-benzoyladenosine (**16**)[11] or a selective di-acylation of adenosine.[12] Whereas **16** was easily prepared (benzoic anhydride, triethylamine, 4-dimethylaminopyridine (DMAP), and acetonitrile at 50 °C), the selective mono-deprotection to **17** was considerably more challenging. Reagents such as hydrazine and hydroxylamine were evaluated, but low conversion was generally observed. Under these conditions, attempts to push the conversion led to indiscriminate deprotection.

On the other hand, the direct di-acylation of adenosine showed more promise (Table 2). Despite the fact that initial screens indicated a tendency toward the formation of the unwanted di-benzoyl isomer **21**, this route was pursued with confidence that **21** could be converted to **17** via acid- or base-mediated isomerization.[12] Overacylation was initially observed even at low temperature (−5 °C); this could be reduced by charging an initial 0.8 equiv of benzoyl chloride followed by additional reagent charges as needed, although incomplete

https://doi.org/10.1021/acs.oprd.1c00026
Org. Process Res. Dev. 2021, 25, 1263−1274

Scheme 5. Strategy for the Alternative Synthesis of 12

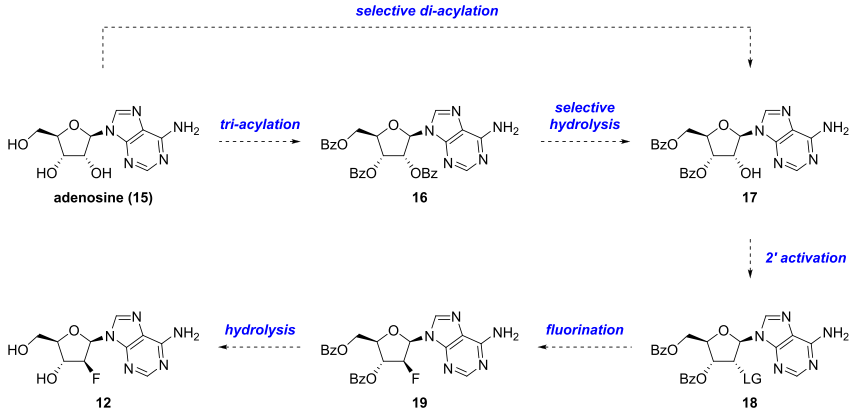

Table 2. Screening Results for the Direct Bis-Acylation of Adenosine

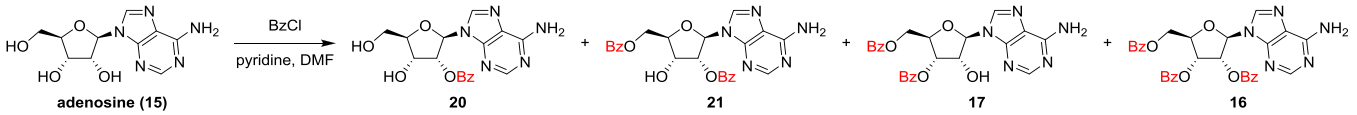

					mono-Bz	di-Bz		tri-Bz
entry	pyridine (vol)	DMF (vol)	BzCl (equiv)	temp. (°C)	20 (% AN)	21 (% AN)	17 (% AN)	16 (% AN)
1	40	25	2.8[a]	−5	24	54	8	10
2	15	10	2.8[a]	−5	28	48	8	11
3	15	10	2.8[a]	10	29	49	9	9
4	15	10	3.0[a]	10	16	53	9	17
5	15	10	2.0[b]	10	13	58	7	18
6	10	5	2.0[b]	10	14	55	6	21

[a]An initial 0.8 equiv of benzoyl chloride was charged, followed by charges of 0.2 equiv. [b]An initial 1.6 equiv of benzoyl chloride was charged over 2 h.

Table 3. Purity of 17 through the Stages of the Benzoylation Process

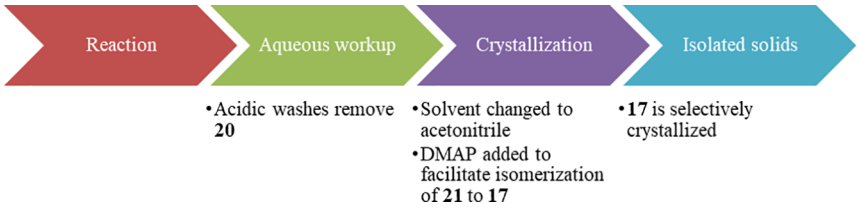

entry	operation	20 (% AN)	21 (% AN)	17 (% AN)	16 (% AN)
1	end of reaction	13	56	6	21
2	after workup	3	43	26	23
3	liquors	6	6	20	55
4	isolated solids	1	0.3	98	0.6

conversion of the monobenzoylated intermediate **20** was observed in this case (entry 1). With portion-wise addition, the solvent charge could be reduced with minimal impact to the reaction profile (entry 2), and the reaction could be warmed to 10 °C as well (entry 3). To increase the reaction conversion, additional benzoyl chloride could be charged (entry 4), although this primarily decreased **20** while increasing the tri-benzoylated impurity **16**. Further improvement was gained by slowly charging 1.6 equiv of benzoyl chloride over 2 h and then charging an additional 0.4 equiv as needed (entry 5), reducing the total quantity of benzoyl chloride required. With these improvements, di-benzoylated isomers **17** and **21** were formed in a combined 60−65% AN (entry 6) favoring regioisomer **21**.[13] As expected, partial isomerization of **21** to **17** via benzoate migration was observed following acidic and basic aqueous washes (Table 3, entries 1 and 2). An additional benefit of washing with acidic solutions is that a significant portion of the monobenzoylated impurity **20** can be purged into the aqueous layer. As potential crystallization conditions were evaluated, it was found that **17** could be crystallized from acetonitrile while rejecting isomer **21**. This discovery, combined with the observed propensity for isomerization in the presence of acid or base, led to the development of a reactive crystallization. After a solvent exchange to acetonitrile, DMAP was added to facilitate isomerization propelled by crystallization of **17** (entries 3 and 4). A purge of the tri-benzoylated impurity **16** was also observed in this crystallization, which provided **17** in 52% yield and >98% AN purity.

https://doi.org/10.1021/acs.oprd.1c00026
Org. Process Res. Dev. 2021, 25, 1263−1274

With access to **17**, the 2′-OH was readily activated as the imidazole-1-sulfonate ester[14] (**22**, Scheme 6). Direct fluorination of **22** with $Et_3N{\cdot}3HF$, however, was complicated with a low yield and the formation of an unexpected migration product (**23**), so alternative approaches were investigated. It was hypothesized that modulation of the electron density in the adenine moiety might suppress its migratory tendency. To test this hypothesis, the N6 nitrogen was acylated with benzoyl chloride, giving **24** (along with a bis-benzoylated impurity at the N6 position; not shown) in 89% isolated yield (Scheme 7).

Scheme 6. Fluorination from 17[a]

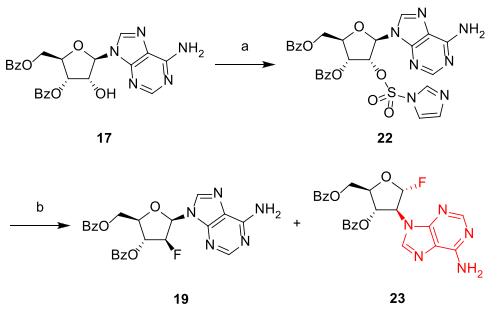

[a]Reagents and conditions: (a) (1) SO_2Cl_2, pyridine, MeTHF, DMF, −10 °C; then, (2) imidazole, MeTHF, −10 to 0 °C, 94%; (b) $Et_3N{\cdot}3HF$, Cy_2NMe, THF, 60 °C, 30−40%, 5:1 (**19**:**23**).

Scheme 7. Revised Fluorination Sequence to 12[a]

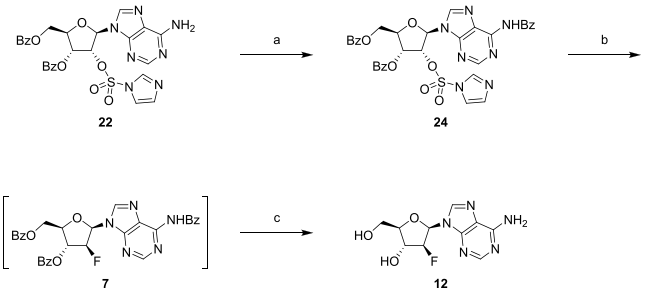

[a]Reagents and conditions: (a) BzCl, NMI, CH_2Cl_2, 0−10 °C, 89%; (b) $Et_3N{\cdot}3HF$, Cy_2NMe, EtOAc, PhMe, 60 °C; and (c) LiOH, MeOH, H_2O, 20 °C, 52% from **24**.

Subjecting **24** to the fluorination reaction provided **7** in 60% yield with no trace of any migration byproducts, albeit with a small amount of the corresponding 2-chloro analogue (the protected precursor of this impurity is formed during the synthesis of **24**); this impurity, however, could be suppressed by conducting the benzoylation at low temperature. Intermediate **7** was then telescoped into the hydrolysis step using the conditions from the route described above to access **12**, with a three-step yield of 46% from **22** (**24** can be crystallized prior to the fluorination reaction, if required). Overall, **12** was obtained in 23% yield (five steps, three to four isolations) from adenosine (**15**) with a purity of >98% AN on several hundred grams scale. Further development of this route will focus on reducing the PMI and the use of chlorinated solvents to lessen the environmental impact of the processes.

Revised Protecting Group Strategy for the Final Steps. With two independent routes to **12** in hand, the development of the downstream processes was addressed. To selectively protect the 3′-OH group, an approach via a diester intermediate was evaluated. From this vantage, enzyme-mediated ester hydrolysis could provide an environmentally friendly route to the desired 3′-ester, particularly as high site-selectivity has been demonstrated in the case of nucleoside diesters.[15] While the use of a benzoyl protecting group would have been ideal as it would allow for the direct use of **7** without the need for hydrolysis and re-protection, initial screening revealed low productivity for this substrate. For the purposes of screening, **8** was acetylated, and the corresponding product **25** was screened across a panel of enzymes (Table 4). Consistent with the known selectivity of these enzymes for nucleoside diester substrates, lipase A from *Candida antarctica* and Amano lipase from *Burkholderia cepacia* primarily formed the regioisomer **27** (entries 1 and 2), while lipase B from *C. antarctica* exhibited a preference for the formation of **26**, albeit with significant overhydrolysis (entry 4). Switching to an immobilized lipase improved the conversion to **26** (entry 6), with Lipolase 100T (entry 7) and NS 99013 (entry 8) giving high conversion and selectivity. The drawback to this approach, however, is that **26** was found to be poorly soluble in most organic solvents. This finding was particularly problematic as the best results for the hydrolysis were achieved using immobilized enzymes and removal of the enzyme after reaction completion via filtration was desired. Fortunately, an improvement in product solubility could be achieved via the replacement of the acetate protecting groups with longer-chain esters. This

Table 4. Enzyme Screening with Substrate 25[a]

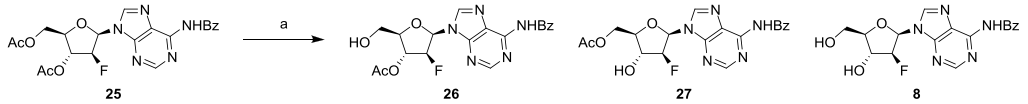

entry	enzyme	25 (% AN)	26 (% AN)	27 (% AN)	8 (% AN)
1	lipase A, *Candida antarctica*	6.1	0	82.8	10.8
2	Amano lipase, *Burkholderia cepacia*, PS	9.4	0.2	83.9	6.5
3	cholesterol esterase, *Pseudomonas fluorescens*	13.8	0	80.9	1.7
4	lipase B, *Candida antarctica*	26.4	16.1	0.3	55.7
5	lipase, *Thermomyces lanuginosus*, solution	72.6	24.3	0.8	0.4
6	lipase, *Thermomyces lanuginosus*, Immobead	0	54.2	0.2	45.6
7	Lipolase 100T[b]	4.3	93.0	0	2.4
8	NS 99013[b]	1.4	96.8	0	1.8

[a]Reagents and conditions: (a) enzyme, dimethyl sulfoxide (DMSO), 0.1 M aqueous sodium phosphate buffer (pH 6.8), ambient temperature, 20 h. [b]Received from Novozymes A/S.

https://doi.org/10.1021/acs.oprd.1c00026
Org. Process Res. Dev. 2021, 25, 1263−1274

Scheme 8. Synthesis of 29 from 12 via Enzyme-Mediated Hydrolysis[a]

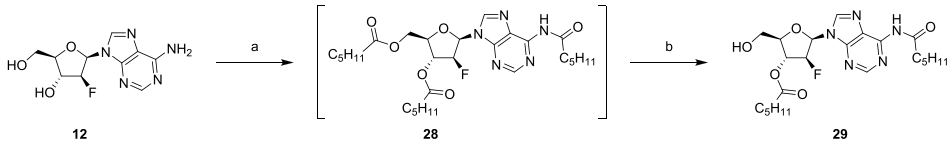

[a]Reagents and conditions: (a) hexanoic anhydride, pyridine, MeCN, 70 °C; (b) Lipolase 100T, MIBK, 0.1 M aqueous sodium phosphate buffer (pH 7), 35 °C, 80% from **12**.

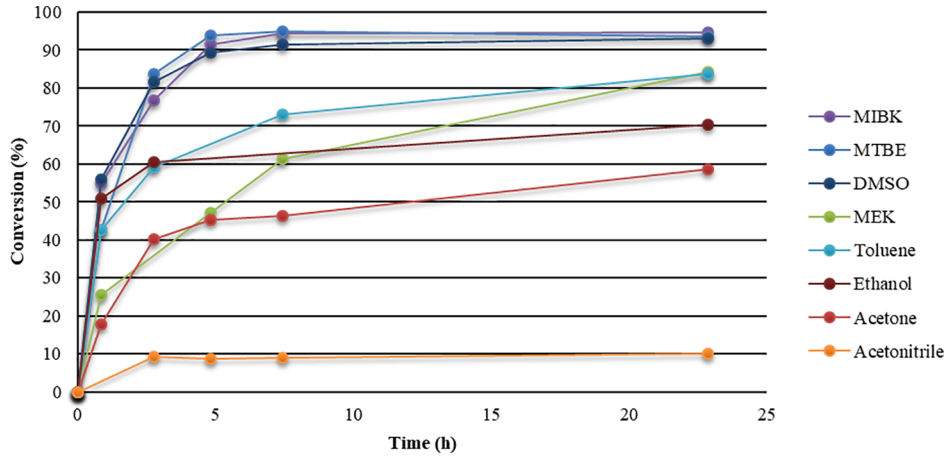

Figure 2. Solvent screen for the hydrolysis of **28** to **29**. Lipolase 100T (20 wt %), organic solvent (10 mL/g), 0.1 M aqueous sodium phosphate buffer (20 mL/g), 35 °C; note: charges are based on the input of **12**.

change in protecting groups had minimal to no impact on the conversion and site-selectivity in the hydrolysis reaction, and ultimately the hexanoate protecting group was selected for further development based on the ready availability of hexanoic anhydride.

With a suitable protecting group selected, reaction conditions were developed to carry out the esterification of **12** and enzymatic hydrolysis of the primary ester as a telescoped sequence (Scheme 8). Intermediate **12** has an additional reactive functional group with the 6-NH_2 moiety as compared to **8**; fortunately, this could be protected concomitantly with the 3′-OH and 5′-OH groups, using hexanoic anhydride (3.6 equiv) and the combination of pyridine as base and acetonitrile as solvent. The selection of pyridine as a base for the reaction was crucial, as use of common alkyl amine bases such as triethylamine led to bis-acylation of the amine.

After aqueous workup, intermediate **28** was subjected to the enzymatic hydrolysis reaction without further purification. During early development, 2-MeTHF was used to facilitate the aqueous workup of **28**, and combining the 2-MeTHF stream with 0.1 M aqueous sodium phosphate buffer (pH 7)[16] and Lipolase 100T (10 wt %) enabled productive conversion to **29** with high site-selectivity (the isomer resulting from hydrolysis at the 3′-position was not detected). The reaction, however, required >40 h to achieve >90% conversion. An evaluation of the initial pH of the reaction (from 6 to 8) revealed an important dependence of the reaction rate on the pH, with lower pH providing a boost to the rate (>90% conversion after 17 h at pH 6). Upon scale-up, however, the reaction conversion ranged from 85 to 95% across trials. To reduce this variability, several alternative organic solvents were tested (Figure 2). From this study, DMSO, *tert*-butyl methyl ether (MTBE), and methyl isobutyl ketone (MIBK) were identified as potential solvents based on the rate of conversion in these cases. DMSO was not pursued further as its miscibility with water would complicate the workup; likewise, MTBE was not evaluated as **29** was found to have low solubility and would precipitate during the reaction, so MIBK was selected for further development. Optimization studies demonstrated that the reaction with MIBK was less sensitive to the initial pH across the range of 6−8. Using the preferred reaction conditions, the solution of **28** in MIBK was combined with 0.1 M aqueous sodium phosphate buffer (pH 7), and then the entire mixture was adjusted to a pH of 7.5 prior to enzyme charging. This protocol allowed for the pH to drift during the reaction (hexanoic acid is produced as a stoichiometric byproduct) while remaining within the desired range. The loading of the enzyme could be reduced to as low as 1 wt %, providing >95% conversion with overnight aging, but a 5 wt % loading was preferred to ensure the robustness of the process. The amount of solvent was also found to influence the reaction conversion, with increased conversion observed at a higher dilution. This trend is likely due to the reaction being an equilibrium between **28** and **29**/hexanoic acid; the hypothesis was supported by the observation that ca. 2% **28** was formed when **29** and hexanoic acid were combined under the reaction conditions. Using 8 mL/g MIBK and 16 mL/g pH 7 buffer consistently provided 95−98% conversion to **29**. After removing the enzyme via filtration and performing an aqueous workup, **29** was crystallized from MIBK and heptane; gratifyingly, this crystallization efficiently purges the unreacted starting material, providing **29** in >98% AN purity. As observed with **12**, hydrogen bonding plays an important role in the crystal lattice of **29** (Figure 3), which may explain the excellent purge of **28** in addition to other process impurities. Overall, **29** was obtained in 80% isolated yield on kilogram scale with a 56% PMI reduction (relative to the synthesis of **10** from **8** in the initial route).

Safe and scalable oxidation conditions were developed for the conversion of silyl ether **10** to intermediate **11** (see the

https://doi.org/10.1021/acs.oprd.1c00026
Org. Process Res. Dev. 2021, 25, 1263−1274

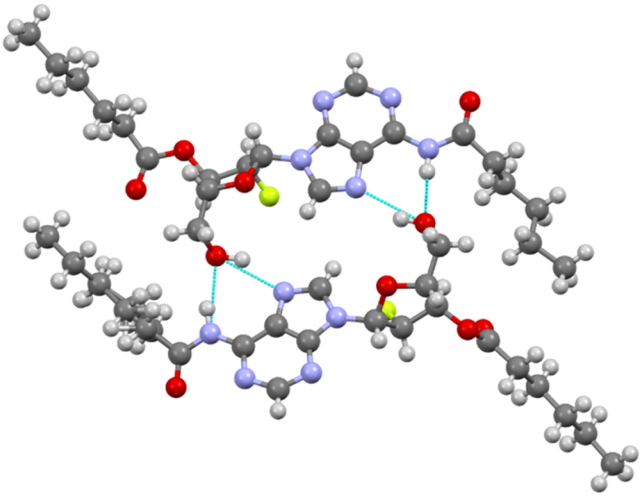

Figure 3. Dimers of **29** via hydrogen bonding (single-crystal X-ray structure).

Supporting Information for reaction calorimetry data), and these conditions were expected to be suitable for the conversion of ester **29** to intermediate **30**; verification was conducted in the laboratory on 65 g scale (Scheme 9). In the oxidation step, the improved solubility of **29** enabled substantial improvement in the reaction throughput via a reduction in solvent usage (60% reduction in acetonitrile, 40% reduction in water). Moreover, the enhanced stability of intermediate **30** allowed for a straightforward aqueous workup. As further scale-up is warranted, additional reaction calorimetry studies will be performed to verify the safety of this revised process. Intermediate **30** is not isolated and is instead carried forward in a telescoped fashion. In the deprotection step, the 3′-ester was found to rapidly undergo solvolysis, followed by cleavage of the hexanamide within 1 h (18−24 h were required for the cleavage of the N^6-benzamide in the initial route). With these process improvements, **1** was obtained in 96% isolated yield (comparable to the initial route) and with a 37% reduction in PMI for the two-step telescoped process.

CONCLUSIONS

In summary, two routes to intermediate **12** were developed and demonstrated on 500 g (or greater) scale, providing manufacturing and supply chain flexibility while reducing the environmental impact of the processes. From **12**, the development of a scalable enzyme-mediated ester hydrolysis enabled a more robust synthesis of **1**. Using the route starting from **4** (Scheme 10), the process improvements increased the yield of **1** by 15% (from 41 to 47%) while reducing the overall PMI by 32% (Figure 4). Organic solvent usage was dramatically reduced (59%), which was partially off-set by a marginal increase in water usage (18%). The increased yield, reduced PMI, and enhancements in operational ease are hallmarks of the new process.

EXPERIMENTAL SECTION

General Information. All reagents were commercially available and used as received. Liquid chromatography (LC) analyses were performed on a Waters Acquity H-Class UPLC system equipped with a photodiode array detector or a Waters Alliance e2695 HPLC system equipped with a photodiode array detector. Purities are reported on an area normalized basis (% AN) as determined by UV detection at the indicated wavelength. NMR analyses were performed on a Bruker 400 MHz AVANCE spectrometer equipped with a 5 mm BBO broadband probe. Chemical shifts for ^{1}H and ^{13}C spectra are reported in ppm relative to tetramethylsilane and were referenced to the solvent residual signal from the deuterated NMR solvent.

LC Methods. Method A (UPLC)—Acquity HSS T3, 1.8 μm, 2.1 mm × 150 mm; 98−10% gradient of 0.1% trifluoroacetic acid (TFA) in water and 0.1% TFA in acetonitrile; flow rate of 0.4 mL/min; column temperature of 30 °C; acquisition time of 24 min; and UV detection at 260 nm.

Method B (HPLC)—Agilent Poroshell 120 EC-C18, 2.7 μm, 4.6 mm × 100 mm; 90−10% gradient of 0.025% TFA in water, and 0.025% TFA in acetonitrile; flow rate of 1.0 mL/min; column temperature of 25 °C; acquisition time of 14 min; and UV detection at 200 nm.

Method C (UPLC)—Acquity HSS T3, 1.8 μm, 2.1 mm × 100 mm; 70−10% gradient of 0.1% formic acid in water and 0.1% formic acid in acetonitrile; flow rate of 0.5 mL/min; column temperature of 30 °C; acquisition time of 13 min; and UV detection at 260 nm.

Method D (UPLC)—Acquity CSH C18, 1.7 μm, 2.1 mm × 150 mm; 95−5% gradient of 0.1% formic acid in water and 0.1% formic acid in acetonitrile; flow rate of 0.4 mL/min; column temperature of 50 °C; acquisition time of 16 min; and UV detection at 260 nm or 274 nm (as indicated).

Method E (UPLC)—Acquity HSS T3, 1.8 μm, 2.1 mm × 100 mm; 70−30% gradient of 0.1% TFA in water and 0.1% TFA in acetonitrile; flow rate of 0.5 mL/min; column temperature of 30 °C; acquisition time of 27 min; and UV detection at 274 nm.

*Preparation of (2R,3R,4S,5R)-5-(6-amino-9H-purin-9-yl)-4-fluoro-2-(hydroxymethyl)tetrahydrofuran-3-ol (**12**) from **4**.* To a reactor were charged **4** (1.5 kg, 3.2 mol) and dichloromethane (5.7 L, 3.8 L/kg). The solution was cooled to 0 °C, and then 33 wt % hydrobromic acid in acetic acid (3.1 kg, 13 mol HBr, 4.0 equiv) was charged while not exceeding an internal temperature of 3 °C; the charge line was rinsed forward with dichloromethane (0.23 L, 0.15 L/kg). The reaction mixture was stirred overnight. Upon reaction completion (determined by ^{19}F NMR), the reaction mixture was diluted with dichloromethane (0.65 L, 0.43 L/kg), and then water (7.5 L, 5.0 L/kg)

Scheme 9. Synthesis of 1 from 29[a]

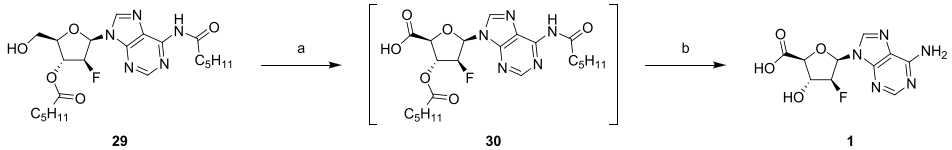

[a]Reagents and conditions: (a) $PhI(OAc)_2$, TEMPO, $Na_2HPO_4{\cdot}7H_2O$, MeCN, H_2O, 22 °C; (b) 25 wt % NaOMe in MeOH, MeOH, 22 °C, 96% from **29**.

https://doi.org/10.1021/acs.oprd.1c00026
Org. Process Res. Dev. 2021, 25, 1263−1274

Scheme 10. Revised Route to 1[a]

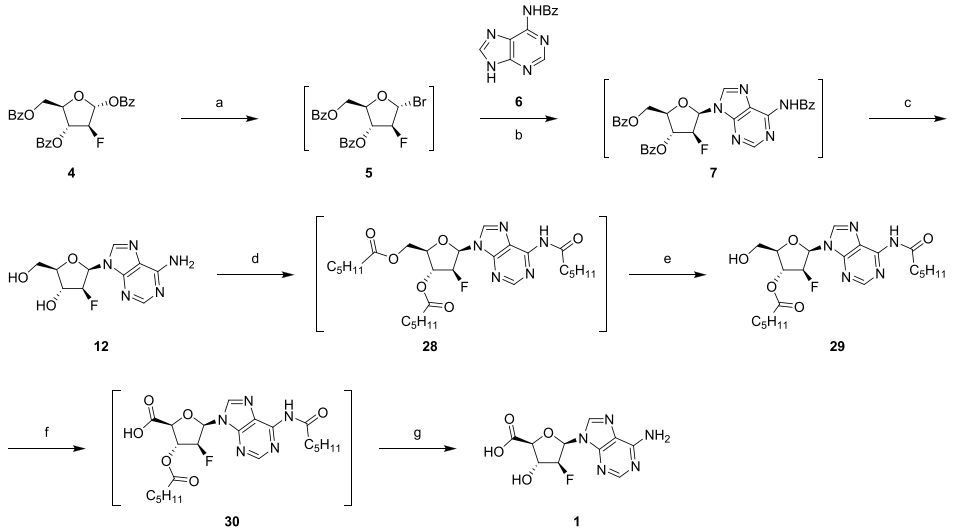

[a]Reagents and conditions: (a) 33 wt % HBr in AcOH, CH_2Cl_2, 0 °C; (b) THF, NMP, 68 °C; (c) LiOH, MeOH, H_2O, 22 °C, 61% from **4**; (d) hexanoic anhydride, pyridine, MeCN, 70 °C; (e) Lipolase 100T, MIBK, 0.1 M aqueous sodium phosphate buffer (pH 7), 35 °C, 80% from **12**; (f) $PhI(OAc)_2$, TEMPO, $Na_2HPO_4{\cdot}7H_2O$, MeCN, H_2O, 22 °C; and (g) 25 wt % NaOMe in MeOH, MeOH, 22 °C, 96% from **29**.

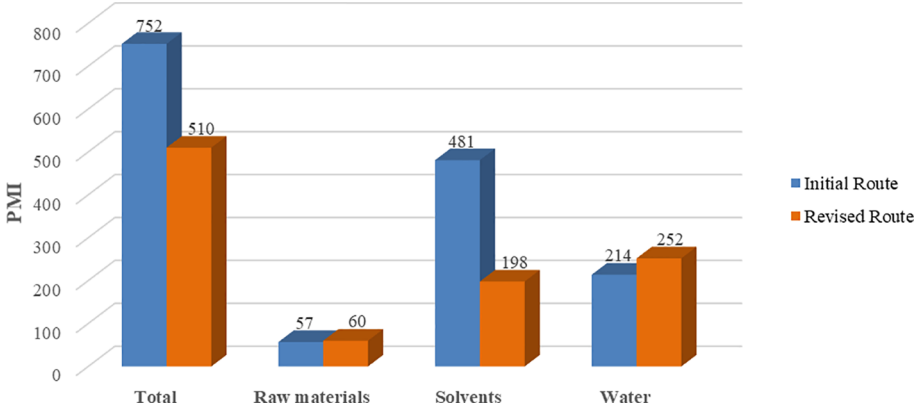

Figure 4. PMI comparison between the initial and revised routes from **4** to **1**.

was charged while not exceeding an internal temperature of 15 °C. The layers were separated, and then the organic layer was washed sequentially with water (7.5 L, 5.0 L/kg) and a solution of sodium carbonate (0.75 kg, 0.50 kg/kg) in water (6.8 L, 4.5 L/kg) while not exceeding an internal temperature of 15 °C. The organic layer was diluted with THF (1.5 L, 1.0 L/kg) and then distilled to a final volume of 3 L (2 L/kg) under vacuum at 35 °C. THF (5.0 L, 3.3 L/kg) was charged, and the resulting solution was distilled to a final volume of 3 L (2 L/kg) under vacuum at 35 °C; this operation was repeated one additional time. The solution was transferred to a separate glass-lined reactor, precharged with **6** (1.7 kg, 7.1 mol, 2.2 equiv), THF (13 L, 8.7 L/kg), and NMP (0.73 L, 0.49 L/kg); the transfer line was rinsed forward with THF (11 L, 7.3 L/kg). The resulting slurry was heated to 68 °C and stirred for 54 h. Upon reaction completion (determined by ^{19}F NMR), the slurry was cooled to ambient temperature and filtered, rinsing forward with THF (1.7 L, 1.1 L/kg), and then the filtrate was returned to the reactor. A solution of sodium chloride (4.0 kg, 2.7 kg/kg) and concentrated hydrochloric acid (1.8 kg, 1.2 kg/kg) in water (33 L, 22 L/kg) was prepared, and then the filtrate was washed three times with the aqueous solutions (the solution was divided into three equal portions). Methanol (7.6 L, 5.1 L/kg) was charged to the organic layer and the solution was adjusted to 22 °C. A solution of lithium hydroxide (0.39 kg, 16 mol, 5.0 equiv) in water (7.8 L, 5.2 L/kg) was charged, and the resulting solution was stirred for 21 h. Upon reaction completion (determined by LC method A), a solution of concentrated hydrochloric acid (2.0 kg, 1.3 kg/kg) in water (1.7 L, 1.1 L/kg) was charged, followed by toluene (7.5 L, 5.0 L/kg). The layers were separated, and the aqueous layer was adjusted to a pH of 6−8 with 25 wt % aqueous sodium hydroxide (1.1 kg, 0.74 kg/kg). The aqueous solution was distilled to a final volume of 14 L (9 L/kg) under vacuum at 50 °C, and a slurry formed during the distillation. The slurry was stirred for 1 h, cooled to 20 °C over 1 h, stirred overnight, and then filtered. The wet cake was washed with water (3.0 L, 2.0 L/kg). The wet cake was dried under vacuum at 50 °C to afford **12** (0.53 kg, 98.7% AN, LC method A) as an off-white solid in 61% yield. ^1H NMR (400 MHz, DMSO-d_6) δ 8.24 (d, J = 2.1 Hz, 1H), 8.16 (s, 1H), 7.34 (s, 2H), 6.41 (dd, J = 14.5, 4.6 Hz, 1H), 5.95 (d, J = 5.0 Hz, 1H), 5.27 (t, J = 4.2 Hz, 0.5H), 5.18−5.07 (m, 1.5H), 4.45 (dtd, J = 18.9, 5.2, 3.8 Hz, 1H), 3.86 (q, J = 4.8 Hz, 1H), and 3.76−3.59 (m, 2H). ^{13}C NMR (101 MHz, DMSO-d_6) δ 156.02, 152.80, 149.16, 139.44 (d, J = 4.1

https://doi.org/10.1021/acs.oprd.1c00026
Org. Process Res. Dev. 2021, 25, 1263−1274

Hz), 118.23, 95.42 (d, J = 192.1 Hz), 83.49 (d, J = 5.3 Hz), 81.43 (d, J = 17.0 Hz), 72.70 (d, J = 23.3 Hz), and 60.43. ^{19}F NMR (376 MHz, DMSO-d_6) δ −197.65 to −197.92 (m). HRMS (ESI +) calculated for $C_{10}H_{13}FN_5O_3^+$ ([M + H]$^+$) 270.09969, found 270.09882.

*Preparation of (2R,3S,4R,5R)-5-(6-amino-9H-purin-9-yl)-2-((benzoyloxy)methyl)-4-hydroxytetrahydrofuran-3-yl benzoate (**17**).* To a reactor were charged adenosine (0.65 kg, 2.4 mol), pyridine (5.9 L, 9.1 L/kg), and DMF (3.3 L, 5.1 L/kg). The resulting slurry was cooled to 9 °C, and then a solution of benzoyl chloride (0.55 kg, 3.9 mol, 1.6 equiv) in pyridine (0.65 L, 1.0 L/kg) was charged over 3 h. The resulting solution was stirred for 1 h; then, additional benzoyl chloride (0.14 kg, 0.98 mol, 0.40 equiv) was charged over 25 min. The reaction mixture was stirred for an additional 1 h. Upon reaction completion (determined by LC method B), the reaction mixture was distilled to a final volume of 3 L (4 L/kg) under vacuum at 75 °C. The reaction mixture was then cooled to 20 °C and dichloromethane (11 L, 17 L/kg) was charged. The reaction mixture was washed with 8 wt % aqueous sodium bicarbonate (6.5 L, 10 L/kg). The layers were separated, and then the organic layer was washed three times with 0.5 M aqueous citric acid (13 L, 20 L/kg; then 2 × 6.5 L, 2 × 10 L/kg). The organic layer was then washed with 8 wt % aqueous sodium bicarbonate (6.5 L, 10 L/kg) followed by water (6.5 L, 10 L/kg). The organic layer was distilled to a final volume of 3 L (4 L/kg) under vacuum at 40 °C. Acetonitrile (3.3 L, 5.1 L/kg) was charged to the reaction mixture, and the resulting solution was distilled to a final volume of 4 L (6 L/kg) under vacuum at 50 °C; this operation was repeated one additional time. The reaction mixture was then heated to reflux (85 °C) and stirred for 1 h giving a slurry. The slurry was cooled to 20 °C, and then DMAP (0.15 kg, 1.2 mol, 0.50 equiv) was charged. The slurry was stirred for 5 h, and then it was cooled to −5 °C over 1 h, stirred overnight, and filtered. The wet cake was washed with cold (−5 °C) acetonitrile (1.3 L, 2.0 L/kg). The wet cake was dried under vacuum at 50 °C to afford **17** (0.60 kg, 97.4% AN, LC method B) as a white solid in 52% yield. ^{1}H NMR (400 MHz, DMSO-d_6) δ 8.37 (s, 1H), 8.12−8.06 (m, 3H), 8.01 (dd, J = 8.3, 1.4 Hz, 2H), 7.75−7.64 (m, 2H), 7.55 (dt, J = 21.4, 7.8 Hz, 4H), 7.34 (s, 2H), 6.07 (dd, J = 11.0, 6.1 Hz, 2H), 5.75 (dd, J = 5.6, 3.5 Hz, 1H), 5.29 (q, J = 6.0 Hz, 1H), and 4.75−4.57 (m, 3H). ^{13}C NMR (101 MHz, DMSO-d_6) δ 165.49, 165.02, 156.14, 152.69, 149.38, 140.09, 133.57, 133.48, 129.53, 129.40, 129.35, 129.29, 128.73, 128.70, 119.32, 87.90, 79.24, 73.19, 70.89, and 63.95. HRMS (ESI+) calculated for $C_{24}H_{22}N_5O_6^+$ ([M + H]$^+$) 476.15646, found 476.15445.

*Preparation of (2R,3R,4R,5R)-4-(((1H-imidazol-1-yl)sulfonyl)oxy)-5-(6-amino-9H-purin-9-yl)-2-((benzoyloxy)methyl)tetrahydrofuran-3-yl benzoate (**22**).* To a reactor were charged **17** (0.58 kg, 1.2 mol), DMF (0.58 L, 1.0 L/kg), pyridine (0.48 kg, 6.1 mol, 5.0 equiv), and 2-MeTHF (3.2 L, 5.5 L/kg). The resulting solution was cooled to −10 °C; then, sulfuryl chloride (0.25 kg, 1.8 mol, 1.5 equiv) was charged over 1 h. The reaction mixture was stirred for an additional 3 h, then a solution of imidazole (0.50 kg, 7.3 mol, 6.0 equiv) in 2-MeTHF (2.6 L, 4.5 L/kg) was charged over 2 h. The solution was warmed to 0 °C and stirred for 14 h. Upon reaction completion (determined by LC method C), 5 wt % aqueous citric acid (2.9 L, 5.0 L/kg) was charged over 30 min. The mixture was warmed to 22 °C, and then the layers were separated. The organic layer was washed with a mixture of water (2.9 L, 5.0 L/kg) and saturated aqueous sodium chloride (0.29 L, 0.50 L/kg). The layers were separated, and the organic layer was distilled to a final volume of 2 L (3 L/kg) under vacuum at 40 °C. 2-MeTHF (5.8 L, 10 L/kg) was charged, and the solution was filtered through a 6 μm filter, rinsing forward with 2-MeTHF (1.2 L, 2.1 L/kg). The filtrate was distilled to a final volume of 5 L (8 L/kg) under vacuum at 40 °C, and then the reaction mixture was adjusted to 30 °C. The solution was seeded with **22** (0.58 g, 0.001 kg/kg). A slurry formed which was stirred for 20 min, and then it was cooled to 20 °C over 30 min. Heptane (2.6 L, 4.5 L/kg) was charged over 8 h, and then the slurry was stirred overnight and filtered. The wet cake was washed with 1:1 2-MeTHF/heptane (2.9 L, 5.0 L/kg). The wet cake was dried under vacuum at 40 °C to afford **22** (0.70 kg, 95.5% AN, LC method C, 6.3 wt % 2-MeTHF) as a light yellow solid in 94% yield. ^{1}H NMR (400 MHz, DMSO-d_6) δ 8.23 (s, 1H), 8.12 (s, 1H), 8.07−8.03 (m, 2H), 8.00−7.96 (m, 2H), 7.82 (s, 1H), 7.77−7.71 (m, 1H), 7.71−7.65 (m, 1H), 7.60 (t, J = 7.8 Hz, 2H), 7.53 (t, J = 7.8 Hz, 2H), 7.49 (t, J = 1.6 Hz, 1H), 7.38 (s, 2H), 6.88−6.83 (m, 1H), 6.49 (dt, J = 10.5, 5.1 Hz, 2H), 6.17 (t, J = 5.2 Hz, 1H), 4.80−4.68 (m, 2H), and 4.58 (dd, J = 12.0, 4.2 Hz, 1H). ^{13}C NMR (101 MHz, DMSO-d_6) δ 165.34, 164.42, 156.11, 152.62, 148.76, 140.25, 137.30, 134.09, 133.49, 130.99, 129.62, 129.32, 129.24, 128.89, 128.66, 128.29, 119.32, 117.98, 85.18, 80.13, 79.10, 69.71, and 62.91. HRMS (ESI+) calculated for $C_{27}H_{24}N_7O_8S^+$ ([M + H]$^+$) 606.14016, found 606.13784.

*Preparation of (2R,3R,4R,5R)-4-(((1H-imidazol-1-yl)sulfonyl)oxy)-5-(6-benzamido-9H-purin-9-yl)-2-((benzoyloxy)methyl)tetrahydrofuran-3-yl benzoate (**24**).* To a reactor were charged **22** (0.67 kg, 1.1 mol), dichloromethane (6.7 L, 10 L/kg), and *N*-methylimidazole (0.41 L, 5.1 mol, 4.6 equiv). The resulting slurry was cooled to 0 °C, and then benzoyl chloride (0.39 L, 3.3 mol, 3.0 equiv) was charged over 1 h. The slurry was warmed to 10 °C and stirred for 3 h, becoming a solution. Upon reaction completion (determined by LC method D at 274 nm), 8 wt % aqueous sodium bicarbonate (6.7 L, 10 L/kg) was charged over 1 h. The mixture was warmed to 20 °C, and then the layers were separated. The aqueous layer was filtered through a pad of diatomaceous earth (0.14 kg, 0.21 kg/kg), rinsing forward with dichloromethane (0.30 L, 0.45 L/kg) to recover an additional organic layer. The combined organic layers were washed with water (6.7 L, 10 L/kg) and the layers were separated. The aqueous layer was filtered through a pad of diatomaceous earth (0.14 kg, 0.21 kg/kg), rinsing forward with dichloromethane (0.30 L, 0.45 L/kg) to recover an additional organic layer. Sodium sulfate (0.67 kg, 1.0 kg/kg) was charged to the combined organic layers, and the resulting slurry was stirred for 30 min. The slurry was filtered, rinsing forward with dichloromethane (0.70 L, 1.0 L/kg). The filtrate was distilled to a final volume of 1 L (2 L/kg) under vacuum at 40 °C. Acetonitrile (3.4 L, 5.1 L/kg) was charged, and the resulting solution was distilled to a final volume of 1 L (2 L/kg) under vacuum at 50 °C; this operation was repeated one additional time. The mixture was cooled to 25 °C, and then water (2.7 L, 4.0 L/kg) was charged over 1 h, giving a slurry. The slurry was stirred for 2 h and filtered. The wet cake was washed with 1:2 acetonitrile/water (1.3 L, 2.0 L/kg) and then water (1.3 L, 2.0 L/kg). The wet cake was dried under vacuum at 50 °C to afford **24** (0.70 kg, 81.9% AN, LC method D at 274 nm) as a light yellow solid in 89% yield. ^{1}H NMR (400 MHz, DMSO-d_6) δ 11.25 (s, 1H), 8.59 (s, 1H), 8.29 (s, 1H), 8.14 (t, J = 1.1 Hz, 1H), 8.10−7.97 (m, 6H), 7.79−7.52 (m, 9H), 7.48 (t, J = 1.5 Hz, 1H), 6.84 (dd, J = 1.8, 0.8 Hz, 1H), 6.66 (d, J = 5.0 Hz, 1H), 6.48 (t, J = 5.4 Hz, 1H), 6.22 (t, J = 5.3 Hz, 1H), 4.87−4.74 (m, 2H),

https://doi.org/10.1021/acs.oprd.1c00026
Org. Process Res. Dev. 2021, 25, 1263−1274

and 4.62 (dd, J = 12.2, 4.3 Hz, 1H). ^{13}C NMR (101 MHz, DMSO-d_6) δ 170.30, 165.59, 165.33, 164.41, 151.53, 151.45, 150.66, 143.75, 137.38, 134.13, 133.54, 133.22, 132.51, 131.13, 129.65, 129.30, 129.27, 128.87, 128.73, 128.51, 128.46, 128.27, 125.97, 117.83, 85.29, 80.09, 79.31, 69.74, 62.87, 59.72, 20.73, and 14.06. HRMS (ESI+) calculated for $C_{34}H_{28}N_7O_9S^+$ ([M + H]$^+$) 710.16637, found 710.16327.

*Preparation of (2R,3R,4S,5R)-5-(6-amino-9H-purin-9-yl)-4-fluoro-2-(hydroxymethyl)tetrahydrofuran-3-ol (**12**) from **24**.* Compound **24** (0.52 kg, 0.73 mol) was divided equally among four round-bottom flasks (0.13 kg, 0.18 mol, each). To each flask was charged ethyl acetate (1.3 L, 10 L/kg, each), toluene (2.0 L, 15 L/kg, each), dicyclohexylmethylamine (79 mL, 0.37 mol, 2.0 equiv, each), and triethylamine trihydrofluoride (0.15 kg, 0.92 mmol, 5.0 equiv, each). The reaction mixtures were heated to 60 °C and stirred for 26 h each. Upon reaction completion (determined by LC method D at 260 nm), the mixtures were cooled to ambient temperature. To each flask, 8 wt % aqueous sodium bicarbonate (1.3 L, 10 L/kg, each) was charged. The layers were separated, and the organic layers were combined in a reactor. The organic layer was washed sequentially with 1 M aqueous hydrochloric acid (5.2 L, 10 L/kg), 8 wt % aqueous sodium bicarbonate (5.2 L, 10 L/kg), and water (5.2 L, 10 L/kg). The organic layer was distilled to a final volume of 0.5 L (1 L/kg) under vacuum at 50 °C. THF (2.6 L, 5.0 L/kg) was charged, and the solution was distilled to a final volume of 0.5 L (1 L/kg) under vacuum at 50 °C. THF (2.6 L, 5.0 L/kg) was charged, and the solution was distilled to a final volume of 2 L (4 L/kg) under vacuum at 50 °C. The mixture was cooled to 20 °C, and then methanol (1.0 L, 2.0 L/kg) was charged. A solution of lithium hydroxide monohydrate (0.054 kg, 1.3 mol, 1.8 equiv) in water (1.1 kg, 2.1 L/kg) was charged while not exceeding an internal temperature of 25 °C. The reaction mixture was then stirred at 20 °C for 16 h. Upon reaction completion (determined by LC method A), 6 M aqueous hydrochloric acid (0.46 kg, 0.88 kg/kg) and toluene (1.0 L, 2.0 L/kg) were charged. The layers were separated, and the aqueous layer was adjusted to a pH of 6−8 with 5 M aqueous sodium hydroxide (0.30 L, 0.57 L/kg). The aqueous solution was distilled to a final volume of 2 L (4 L/kg) under vacuum at 50 °C, and a slurry formed during the distillation. The slurry was cooled to 20 °C over 1 h, stirred for an additional 1 h, and then filtered. The wet cake was washed with water (0.41 L, 0.79 L/kg). The wet cake was dried under vacuum at 50 °C to afford **12** (0.10 kg, 98.6% AN, LC method A) as a light tan solid in 52% yield. ^{1}H NMR (400 MHz, DMSO-d_6) δ 8.24 (d, J = 2.1 Hz, 1H), 8.16 (s, 1H), 7.34 (s, 2H), 6.41 (dd, J = 14.6, 4.6 Hz, 1H), 5.95 (d, J = 5.1 Hz, 1H), 5.27 (t, J = 4.2 Hz, 0.5H), 5.15−5.09 (m, 1.5H), 4.45 (dtd, J = 18.9, 5.2, 3.8 Hz, 1H), 3.85 (q, J = 4.9 Hz, 1H), and 3.76−3.59 (m, 2H). ^{13}C NMR (101 MHz, DMSO-d_6) δ 156.02, 152.79, 149.16, 139.44 (d, J = 4.0 Hz), 118.23, 95.41 (d, J = 192.0 Hz), 83.48 (d, J = 5.4 Hz), 81.43 (d, J = 17.0 Hz), 72.70 (d, J = 23.2 Hz), and 60.43. ^{19}F NMR (376 MHz, DMSO-d_6) δ −197.66 to −197.93 (m). HRMS (ESI+) calculated for $C_{10}H_{13}FN_5O_3^+$ ([M + H]$^+$) 270.09969, found 270.09867.

*Preparation of (2R,3R,4S,5R)-4-fluoro-5-(6-hexanamido-9H-purin-9-yl)-2-(hydroxymethyl)tetrahydrofuran-3-yl hexanoate (**29**).* To a reactor were charged **12** (1.3 kg, 4.7 mol), acetonitrile (3.8 L, 3.0 L/kg), pyridine (1.5 kg, 19 mol, 4.1 equiv), and hexanoic anhydride (3.7 kg, 17 mol, 3.7 equiv). The resulting slurry was heated to 70 °C and stirred for 21 h, to give a solution. Upon reaction completion (determined by LC method E), the reaction mixture was cooled to 35 °C, and then MIBK (10 L, 8.0 L/kg) was charged. The solution was washed three times with saturated aqueous sodium bicarbonate (7.2 kg, 5.7 kg/kg, each). The organic layer was combined with 0.1 M aqueous sodium phosphate buffer (pH 7, 20 kg, 16 kg/kg). The resulting mixture was adjusted to 35 °C and to a pH of 7.5 with 50 wt % aqueous sodium hydroxide (1.7 kg, 1.4 kg/kg). Lipolase 100T (63.0 g, 0.05 kg/kg) was charged, and the reaction mixture was stirred for 25 h. Upon reaction completion (determined by LC method E), the reaction mixture was filtered through a pad of diatomaceous earth (0.64 kg, 0.51 kg/kg), rinsing forward twice with MIBK (1.3 L, 1.0 L/kg, each). The filtrate was returned to the reactor, and the layers were separated. The organic layer was washed sequentially with saturated aqueous sodium bicarbonate (8.4 kg, 6.7 kg/kg) and 0.1 M aqueous sodium phosphate buffer (pH 7, 7.5 kg, 6.0 kg/kg). The organic layer was filtered through a 1.2 μm filter, rinsing forward with MIBK (0.62 L, 0.50 L/kg). The filtrate was distilled to a final volume of 5 L (4 L/kg) under vacuum at 50 °C. The solution was adjusted to 45 °C, and heptane (2.6 L, 2.0 L/kg) was charged over 1 h. The mixture was seeded with **29** (6.2 g, 0.005 kg/kg), and then additional heptane (7.6 L, 6.0 L/kg) was charged over 3 h to give a slurry. The slurry was cooled to 20 °C over 5 h, stirred overnight, and filtered. The wet cake was washed with 1:4 MIBK/heptane (2.5 L, 2.0 L/kg). The wet cake was dried under vacuum at 40 °C to afford **29** (1.7 kg, 98.8% AN, LC method E) as a white solid in 80% yield. ^{1}H NMR (400 MHz, DMSO-d_6) δ 10.72 (s, 1H), 8.68 (s, 1H), 8.59 (d, J = 2.4 Hz, 1H), 6.56 (dd, J = 17.1, 4.1 Hz, 1H), 5.60−5.55 (m, 1H), 5.49 (ddd, J = 24.1, 4.6, 2.6 Hz, 1H), 5.19 (t, J = 5.9 Hz, 1H), 4.11 (q, J = 4.6 Hz, 1H), 3.71 (ddt, J = 23.6, 11.9, 6.5 Hz, 2H), 2.56 (t, J = 7.4 Hz, 2H), 2.42 (t, J = 7.4 Hz, 2H), 1.67−1.52 (m, 4H), 1.37−1.23 (m, 8H), and 0.93−0.82 (m, 6H). ^{13}C NMR (101 MHz, DMSO-d_6) δ 172.14, 171.59, 151.98, 151.44, 149.73, 142.70 (d, J = 4.8 Hz), 122.96, 93.15 (d, J = 192.3 Hz), 82.08 (d, J = 16.9 Hz), 81.49 (d, J = 3.4 Hz), 74.86 (d, J = 27.5 Hz), 60.37, 36.08, 33.16, 30.78, 30.56, 24.37, 23.87, 21.88, 21.75, 13.83, and 13.77. ^{19}F NMR (376 MHz, DMSO-d_6) δ −197.26 to −197.53 (m). HRMS (ESI+) calculated for $C_{22}H_{33}FN_5O_5^+$ ([M + H]$^+$) 466.24602, found 466.24390.

*Preparation of (2S,3R,4S,5R)-5-(6-amino-9H-purin-9-yl)-4-fluoro-3-hydroxytetrahydrofuran-2-carboxylic acid (**1**).* To a reactor were charged **29** (65 g, 140 mmol), sodium phosphate dibasic heptahydrate (220 g, 810 mmol, 5.8 equiv), acetonitrile (330 mL, 5.0 L/kg), and water (330 mL, 5.0 L/kg). To the resulting slurry, iodobenzene diacetate (120 g, 380 mmol, 2.7 equiv) was charged followed by TEMPO (3.3 g, 21 mmol, 0.15 equiv), resulting in an exotherm from 15 to 29 °C over 10 min and giving a biphasic solution. The reaction mixture was stirred at 22 °C for an additional 40 min. Upon reaction completion (determined by LC method E), a solution of sodium sulfite (13 g, 100 mmol, 0.74 equiv) in water (120 mL, 1.8 L/kg) was charged over 5 min. The mixture was stirred for 15 min at 22 °C and then tested for residual oxidant (potassium iodide starch test paper). 2-MeTHF (260 mL, 4.0 L/kg) was charged and the layers were separated. The aqueous layer was extracted with 2-MeTHF (130 mL, 2.0 L/kg). The combined organic layers were returned to the reactor, rinsing forward with 2-MeTHF (33 mL, 0.51 L/kg), and washed twice with 15 wt % aqueous sodium chloride solution (330 mL, 5.0 L/kg, each). The organic layer was distilled to a final volume of 450 mL (6 L/kg) under vacuum at 50 °C. Methanol (420 mL, 6.4 L/kg) was charged and the resulting solution was distilled to a final volume of 330 mL (5 L/kg) under vacuum at 55 °C. The solution was cooled to 22 °C,

https://doi.org/10.1021/acs.oprd.1c00026
Org. Process Res. Dev. 2021, 25, 1263−1274

and then methanol (81 mL, 1.2 L/kg) and 25 wt % sodium methoxide in methanol (69 mL, 300 mmol, 2.2 equiv) were charged. The reaction mixture was stirred at 22 °C for 5 h. Upon reaction completion (determined by LC method A), a solution of sodium chloride (16 g, 0.25 kg/kg) in water (310 mL, 4.8 L/kg) was charged followed by *tert*-butyl methyl ether (440 mL, 6.8 L/kg). The resulting mixture was heated to 42 °C, and the pH was adjusted to 3 with 6 M aqueous hydrochloric acid solution to give a slurry. The slurry was cooled to 20 °C over 1 h, stirred overnight, and filtered. The wet cake was washed with MTBE (88 mL, 1.4 L/kg), twice with water (65 mL, 1.0 L/kg, each), and finally with THF (74 mL, 1.1 L/kg). The wet cake was dried under vacuum at 50 °C to afford **1** (38 g, 99.4% AN, LC method A) as a white solid in 96% yield. ^{1}H NMR (400 MHz, DMSO-d_6) δ 13.83 (br, exchangeable), 8.34 (d, J = 2.6 Hz, 1H), 8.18 (s, 1H), 7.44 (br, 2H), 6.58 (dd, J = 23.7, 2.9 Hz, 1H), 6.48 (br, 1H), 5.12 (ddd, J = 50.3, 3.0, 1.5 Hz, 1H), 4.71−4.65 (m, 1H), 4.61 (d, J = 1.2 Hz, 1H). ^{13}C NMR (101 MHz, DMSO-d_6) δ 170.90, 156.11, 152.60, 148.72, 139.90 (d, J = 4.4 Hz), 118.27, 93.01 (d, J = 189.6 Hz), 84.97 (d, J = 15.3 Hz), 83.01, and 76.62 (d, J = 26.0 Hz). ^{19}F NMR (376 MHz, DMSO-d_6) δ −197.61 (dddd, J = 50.3, 23.6, 10.1, 2.7 Hz). HRMS (ESI +) calculated for $C_{10}H_{11}FN_5O_4^+$ ([M + H]$^+$) 284.07896, found 284.07815.

■ ASSOCIATED CONTENT

Supporting Information

The Supporting Information is available free of charge at https://pubs.acs.org/doi/10.1021/acs.oprd.1c00026.

Reaction calorimetry and representative experimental procedure for the conversion of **10** to **1** (PDF)

Crystallographic data of **12** (CIF)

Crystallographic data of **29** (CIF)

■ AUTHOR INFORMATION

Corresponding Author

David A. Siler − *Department of Process Chemistry, Gilead Sciences, Inc., Foster City, California 94404, United States;* orcid.org/0000-0002-2642-4392; Email: david.siler@gilead.com

Authors

Selcuk Calimsiz − *Department of Process Development, Gilead Alberta ULC, Edmonton, Alberta T6S 1A1, Canada*

Ian J. Doxsee − *Department of Process Chemistry, Gilead Sciences, Inc., Foster City, California 94404, United States*

Bernard Kwong − *Department of Process Development, Gilead Alberta ULC, Edmonton, Alberta T6S 1A1, Canada*

Jeffrey D. Ng − *Department of Process Chemistry, Gilead Sciences, Inc., Foster City, California 94404, United States*

Keshab Sarma − *Department of Process Chemistry, Gilead Sciences, Inc., Foster City, California 94404, United States*

Jinyu Shen − *Department of Process Development, Gilead Alberta ULC, Edmonton, Alberta T6S 1A1, Canada*

Jonah W. Curl − *Department of Process Development, Gilead Alberta ULC, Edmonton, Alberta T6S 1A1, Canada*

Jason A. Davy − *Department of Process Development, Gilead Alberta ULC, Edmonton, Alberta T6S 1A1, Canada*

Jeffrey A. O. Garber − *Department of Process Development, Gilead Alberta ULC, Edmonton, Alberta T6S 1A1, Canada*

Sura Ha − *Pharmaceutical Process R&D Team, Research Institute, Yuhan Corporation, Yongin-si 17084, Gyeonggi-do, South Korea*

Olga Lapina − *Department of Process Chemistry, Gilead Sciences, Inc., Foster City, California 94404, United States*

Jisung Lee − *Pharmaceutical Process R&D Team, Research Institute, Yuhan Corporation, Yongin-si 17084, Gyeonggi-do, South Korea*

Lennie Lin − *Department of Process Development, Gilead Alberta ULC, Edmonton, Alberta T6S 1A1, Canada*

Sangsun Park − *Pharmaceutical Process R&D Team, Research Institute, Yuhan Corporation, Yongin-si 17084, Gyeonggi-do, South Korea*

Mary Rosario − *Department of Process Development, Gilead Alberta ULC, Edmonton, Alberta T6S 1A1, Canada*

Olivier St-Jean − *Department of Process Chemistry, Gilead Sciences, Inc., Foster City, California 94404, United States*

Guojun Yu − *Department of Process Development, Gilead Alberta ULC, Edmonton, Alberta T6S 1A1, Canada*

Complete contact information is available at: https://pubs.acs.org/10.1021/acs.oprd.1c00026

Author Contributions

The manuscript was written through the contributions of all authors. All authors have given approval to the final version of the manuscript.

Notes

The authors declare the following competing financial interest(s): The authors are employees of Gilead Sciences, Inc., Foster City, California, United States; Gilead Alberta ULC, Edmonton, Alberta, Canada; and Yuhan Corporation, Yongin, Gyeonggi, South Korea.

■ ACKNOWLEDGMENTS

The authors would like to thank Li Wang for experimental contributions, Amy Cagulada, Nisha Shah, and Lu Zou for performing reaction safety assessments, Sunghee Cho, Teague McGinitie, Sebin Park, and Alban Pereira for analytical support, and Andrea Ambrosi and Dietrich Steinhuebel for helpful feedback on the manuscript.

■ REFERENCES

(1) (a) Seley-Radtke, K. L.; Yates, M. K. The evolution of nucleoside analogue antivirals: A review for chemists and non-chemists. Part 1: Early structural modifications to the nucleoside scaffold. *Antivir. Res.* **2018**, *154*, 66−86. (b) Yates, M. K.; Seley-Radtke, K. L. The evolution of antiviral nucleoside analogues: A review for chemists and non-chemists. Part II: Complex modifications to the nucleoside scaffold. *Antivir. Res.* **2019**, *162*, 5−21.

(2) Zhou, Y.; Wang, J.; Gu, Z.; Wang, S.; Zhu, W.; Aceña, J. L.; Soloshonok, V. A.; Izawa, K.; Liu, H. Next Generation of Fluorine-Containing Pharmaceuticals, Compounds Currently in Phase II-III Clinical Trials of Major Pharmaceutical Companies: New Structural Trends and Therapeutic Areas. *Chem. Rev.* **2016**, *116*, 422−518.

(3) (a) Cavaliere, A.; Probst, K. C.; Westwell, A. D.; Slusarczyk, M. Fluorinated nucelosides as an important class of anticancer and antiviral agents. *Future Med. Chem.* **2017**, *9*, 1809−1833. (b) Liu, P.; Sharon, A.; Chu, C. K. Fluorinated nucleosides: Synthesis and biological implication. *J. Fluorine Chem.* **2008**, *129*, 743−766.

(4) (a) Boojamra, C. G.; Mackman, R. L.; Markevitch, D. Y.; Prasad, V.; Ray, A. S.; Douglas, J.; Grant, D.; Kim, C. U.; Cihlar, T. Synthesis and anti-HIV activity of GS-9148 (2′-Fd4AP), a novel nucleoside phosphonate HIV reverse transcriptase inhibitor. *Bioorg. Med. Chem. Lett.* **2008**, *18*, 1120−1123. (b) Ray, A. S.; Vela, J. E.; Boojamra, C. G.;

Zhang, L.; Hui, H.; Callebaut, C.; Stray, K.; Lin, K.-Y.; Gao, Y.; Mackman, R. L.; Cihlar, T. Intracellular Metabolism of the Nucleotide Prodrug GS-9131, a Potent Anti-Human Immunodeficiency Virus Agent. *Antimicrob. Agents Chemother.* **2008**, *52*, 648−654. (c) Boojamra, C. G.; Lin, K.-Y.; Mackman, R.; Markevitch, D. Y.; Petrakovsky, O. V.; Ray, A. S.; Zhang, L. Phosphonate Analogs of HIV Inhibitor Compounds. U.S. Patent US7871991 B22011.

(5) (a) Standley, E. A.; Bringley, D. A.; Calimsiz, S.; Ng, J. D.; et al. Synthesis of Rovafovir Etalafenamide (Part I): Active Pharmaceutical Ingredient Process Development, Scale-Up, and Impurity Control Strategy *Org. Process Res. Dev.* **2021**, accepted for publication. DOI: 10.1021/acs.oprd.1c00059. (b) Ambrosi, A.; Bringley, D. A.; Calimsiz, S.; Garber, J. A. O.; et al. Synthesis of Rovafovir Etalafenamide (Part III): Evolution of the Synthetic Process to the Phosphonamidate Fragment *Org. Process Res. Dev.* **2021**, DOI: 10.1021/acs.oprd.0c00428.

(6) Yu, R. H. C.; Brown, B. H.; Polniaszek, R. P.; Graetz, B. R.; Sujino, K.; Tran, D. D.-P.; Triman, A. S.; Kent, K. M.; Pfeiffer, S. Processes and Intermediates for Preparing Anti-HIV Agents. WIPO Patent WO2012US38615.

(7) (a) Tann, C. H.; Brodfuehrer, P. R.; Brundidge, S. P.; Sapino, C., Jr.; Howell, H. G. Fluorocarbohydrates in Synthesis. An Efficient Synthesis of 1-(2-Deoxy-2-fluoro-β-D-arabinofuranosyl)-5-iodouracil (β-FIAU) and 1-(2-Deoxy-2-fluoro-β-D-arabinofuranosyl)thymine (β-FMAU). *J. Org. Chem.* **1985**, *50*, 3644−3647. (b) Chou, T. S.; Becke, L. M.; O'Toole, J. C.; Carr, M. A.; Parker, B. E. Triethylamine poly(hydrogen fluorides) in the synthesis of a fluorinated nucleoside glycon. *Tetrahedron Lett.* **1996**, *37*, 17−20.

(8) Jimenez-Gonzalez, C.; Ponder, C. S.; Broxterman, Q. B.; Manley, J. B. Using the Right Green Yardstick: Why Process Mass Intensity is Used in the Pharmaceutical Industry to Drive More Sustainable Processes. *Org. Process Res. Dev.* **2011**, *15*, 912−917.

(9) (a) Bauta, W. E.; Schulmeier, B. E.; Burke, B.; Puente, J. F.; Cantrell, W. R., Jr.; Lovett, D.; Goebel, J.; Anderson, B.; Ionescu, D.; Guo, R. A New Process for Antineoplastic Agent Clofarabine. *Org. Process Res. Dev.* **2004**, *8*, 889−896. (b) Tann, C. H.; Brodfuehrer, P. R.; Brundidge, S. P.; Sapino, C., Jr.; Howell, H. G. Fluorocarbohydrates in Synthesis. An Efficient Synthesis of 1-(2-Deoxy-2-fluoro-β-D-arabinofuranosyl)-5-iodouracil (β-FIAU) and 1-(2-Deoxy-2-fluoro-β-D-arabinofuranosyl)thymine (β-FMAU). *J. Org. Chem.* **1985**, *50*, 3644−3647. It is also possible that the increasing solvent polarity increases the solubility of bromide which could racemize the anomeric position prior to displacement; for example: (c) Kotick, M. P.; Szantay, C.; Bardos, T. J. Synthesis of 5-*S*-Substituted 2′-Deoxyuridines. Study of the Factors Influencing the Stereoselectivity of the Silyl Modification of the Hilbert-Johnson Reaction. *J. Org. Chem.* **1969**, *34*, 3806−3813. For an alternative strategy for glycosylation with poorly soluble bases, see: (d) Gallou, F.; Seeger-Weibel, M.; Chassagne, P. Development of a Robust and Sustainable Process for Nucleoside Formation. *Org. Process Res. Dev.* **2013**, *17*, 390−396.

(10) The diastereomeric ratio typically observed in vial-scale screening experiments was slightly lower than the ratio observed on scale.

(11) (a) Kumar, P.; Emami, S.; Kresolek, Z.; Yang, J.; McEwan, A.; Wiebe, L. Synthesis and Hypoxia Selective Radiosensitization Potential of β-2-FAZA and β-3-FAZL: Fluorinated Azomycin β-Nucleosides. *Med. Chem.*. **2009**, *5*, 118−129. (b) Kirschberg, T. A.; Mish, M.; Squires, N. H.; Zonte, S.; Aktoudianakis, E.; Metobo, S.; Butler, T.; Ju, X.; Cho, A.; Ray, A. S.; Kim, C. U. Synthesis of 1′- C -Cyano Pyrimidine Nucleosides and Characterization as HCV Polymerase Inhibitors. *Nucleosides, Nucleotides and Nucleic Acids* **2015**, *34*, 763−785. (c) Xu, S.; Yao, P.; Chen, G.; Wang, H. A New Synthesis of 2-Chloro-2′-Deoxyadenosine (Cladribine), CdA). *Nucleosides, Nucleotides and Nucleic Acids* **2011**, *30*, 353−359.

(12) (a) Sivets, G. G. Regio- and Stereoselective Syntheses of l-Pentose Derivatives from l-Arabinose. *Tetrahedron* **2018**, *74*, 920−931. (b) Simeó, Y.; Sinisterra, J. V.; Alcántara, A. R. Regioselective Enzymatic Acylation of Pharmacologically Interesting Nucleosides in 2-Methyltetrahydrofuran, a Greener Substitute for THF. *Green Chem.* **2009**, *11*, 855−862. (c) Jones, L. A.; Moorman, A. R.; Chamberlain, S. D.; de Miranda, P.; Reynolds, D. J.; Burns, C. L.; Krenitsky, T. A. Di- and Triester Prodrugs of the Varicella-Zoster Antiviral Agent 6-Methoxypurine Arabinoside. *J. Med. Chem.* **1992**, *35*, 56−63.

(13) Although 10 volumes of pyridine are still required for this reaction, a majority can be recovered via distillation and recycled.

(14) Yoshimura, Y.; Endo, M.; Miura, S.; Sakata, S. An Alternative Synthesis of the Antineoplastic Nucleoside 4′-ThioFAC and Its Application to the Synthesis of 4′-ThioFAG and 4′-Thiocytarazid. *J. Org. Chem.* **1999**, *64*, 7912−7920.

(15) (a) García, J.; Fernández, S.; Ferrero, M.; Sanghvi, Y. S.; Gotor, V. Building Blocks for the Solution Phase Synthesis of Oligonucleotides: Regioselective Hydrolysis of 3′,5′-Di-*O*-levulinylnucleosides Using an Enzymatic Approach. *J. Org. Chem.* **2002**, *67*, 4513−4519. (b) Taverna-Porro, M.; Bouvier, L. A.; Pereira, C. A.; Montserrat, J. M.; Iribarren, A. M. Chemoenzymatic Preparation of Nucleosides from Furanoses. *Tetrahedron Lett.* **2008**, *49*, 2642−2645. (c) Martínez-Montero, S.; Fernández, S.; Sanghvi, Y. S.; Gotor, V.; Ferrero, M. An Expedient Biocatalytic Procedure for Abasic Site Precursors Useful in Oligonucleotide Synthesis. *Org. Biomol. Chem.* **2011**, *9*, 5960−5966.

(16) Prepared from sodium phosphate monobasic and sodium phosphate dibasic.

https://doi.org/10.1021/acs.oprd.1c00026
Org. Process Res. Dev. 2021, 25, 1263−1274